Journal of Alloys and Compounds 509S (2011) S775–S778

Contents lists available at ScienceDirect

Journal of Alloys and Compounds

journal homepage: www.elsevier.com/locate/jallcom

# Hydrogenation and microstructural study of melt-spun $Ti_{0.8}V_{0.2}$

S. Suwarno[a,*], J.K. Solberg[a], V.A. Yartys[a,b], B. Krogh[c]

[a] Department of Materials Science and Engineering, NTNU, Alfred Getz Vei 2, NO-7491 Trondheim, Norway
[b] Institute for Energy Technology, P.O. Box 40, NO-2027 Kjeller, Norway
[c] Statoil Research Centre, Rotvoll, N-7005 Trondheim, Norway

ARTICLE INFO

*Article history:*
Received 12 July 2010
Received in revised form 22 October 2010
Accepted 22 October 2010
Available online 4 November 2010

*Keywords:*
Metal hydrides
Rapid-solidification
Microstructure
SEM

ABSTRACT

In this work we utilized the melt spinning process to prepare a nanostructured $Ti_{0.8}V_{0.2}$ alloy for hydrogen storage applications. The alloy ribbons were solidified from the melt using two different wheel spinner velocities, 1000 and 3000 rpm. LOM, and SEM were utilized to examine the microstructures of the ribbons and their corresponding hydrides. Hydrogen absorption and desorption experiments were performed using a TDS setup. Arc melted $Ti_{0.8}V_{0.2}$ and rapidly solidified (RS) materials (RS1000 and RS3000) formed FCC dihydrides with lattice parameters ranging from 4.4198 to 4.4338 Å. RS resulted in a dramatic decrease of the grain size, down to smaller than 200 nm for the hydrogenated $Ti_{0.8}V_{0.2}$ RS3000 alloy. The thermal stability of the hydrides was strongly affected by the RS solidification rate. For the hydride of $Ti_{0.8}V_{0.2}$ RS3000, a significant decrease in the thermal stability was observed, so the peak of hydrogen desorption was shifted to much lower temperatures, by ~80 °C, as compared to the hydrogenated as cast alloy.



## 1. Introduction

Titanium, vanadium and their alloys have high hydrogen gravimetric and volumetric absorption capacities reaching ~4 wt.% H or 150 kg H/m$^3$. The hydrogenation process is very exothermic. Hence, these alloys are promising candidates for hydrogen and heat storage applications, particularly in stationary systems. Both the H storage capacities and the hydrogenation enthalpies may be modified by changing the content of vanadium, or by adding a third component, including different transition elements, to the binary Ti–V alloys crystallizing with the BCC-type crystal structures with the highest values of hydrogen densities [1–3]. This possibility is very useful when specific operating working temperatures are to be optimized. Further to the modification of the chemical composition, a convenient way to control the properties is by selecting and optimizing the conditions of the synthesis process.

As the chemical element distribution, the crystal structure, and the microstructure of an as cast alloy are all determined by the solidification rate, the rapid solidification (RS) process can be applied to produce optimized microstructures, by effectively controlling this parameter. Rapid solidification/rapid quenching is especially beneficial for the Ti-based alloys because it suppresses the formation of the phases other than the BCC alloy [4,5]. In addition, homogeneous element distribution may be achieved. Thus, better control over the equilibrium pressures of hydrogen absorption–desorption can be obtained [6]. Furthermore, RS has been found to improve cycling properties of the hydrides [7,8]. Melt spinning is one type of the RS technique which has being used for optimizing the microstructures of the Ti–V based alloys [6,9] as well as for producing the nanostructured Mg–Mm–Ni composites [10]. In the present work, we have utilized the melt spinning process to further modify the hydrogen sorption properties of the Ti–V alloys. The aim was in studying the morphology and microstructure of the $Ti_{0.8}V_{0.2}$ alloys and their hydrides and relating them to the hydrogen absorption–desorption behaviour of the alloy, in order to propose the ways of optimizing the preparation route.

### 2. Experimental procedure

The as cast $Ti_{0.8}V_{0.2}$ used for rapid solidification was prepared by arc melting the individual metals, Ti and V (both having purity of 99.9%), in argon gas. The sample with the mass of 10 g was turned over and remelted several times to achieve a better homogeneity. This button-shaped sample was then cut into pieces for the preparation of the ribbons during the melt spinning performed in argon gas. Two different copper wheel spinner velocities were employed, i.e. 1000 and 3000 rpm. The morphology and microstructure of the ribbons were characterized by light optical microscopy (LOM) and field emission SEM. Hydrogenation and dehydrogenation were done in the Sieverts type TDS setup. The ribbons were activated by heating in vacuum to 600 °C with a dwell time of 30 min, followed by cooling to room temperature. First hydrogenation was performed at initial hydrogen pressure of 6 bar by heating the sample from room temperature to 400 °C with a heating rate of 5 K/min. Thermal Desorption Spectroscopy (TDS) was conducted in dynamic vacuum (with starting pressure of ~$1 \times 10^{-5}$ mbar), using a constant heating rate of 5 K/min in a temperature interval from room temperature to 800 °C. Subsequent rehydrogenation was performed at 30 °C at hydrogen pressure of 6 bar. To achieve higher accuracy, the mass of the sample used in each measurement was

* Corresponding author. Tel.: +47 7394868.
*E-mail address:* suwarno@material.ntnu.no (S. Suwarno).

0925-8388/$ – see front matter © 2010 Elsevier B.V. All rights reserved.
doi:10.1016/j.jallcom.2010.10.130

0.5–1 g. The crystal structure data were evaluated using Synchrotron X-ray diffraction performed at the beam station BM1A accommodated at the Swiss-Norwegian Beam Lines, European Synchrotron Research Facility, Grenoble, France with the wavelength of $\lambda = 0.72085$ Å. The samples were placed into quartz glass capillaries (0.5 mm in diameter and 0.1 mm wall thickness).

## 3. Results and discussion

An arc melted $Ti_{0.8}V_{0.2}$ was found to crystallize with a BCC crystal structure (space group $Im\bar{3}m$), with a unit cell parameter of 3.2298 Å. The melt spinning produced ribbons of different thickness, which decreased with increasing the wheel spinner velocity, being approximately 53.4 μm for RS1000 and 20.3 μm for RS3000. Changes in the thickness of the ribbons are because of an inverse proportional dependence of the thickness and the solidification rate. The microstructures of the ribbons were studied by LOM and SEM. An average grain size of the BCC phase in the $Ti_{0.8}V_{0.2}$ ribbons was 20.1 μm for RS1000 and 5.3 μm for RS3000. A decrease in the grain size with increasing solidification rate was expected and was observed earlier [11,12].

Hydrogenation of the ribbons was performed after degassing of the sample by heating it from room temperature to 600 °C in vacuum. During the hydrogen absorption experiment, the sample was heated from RT to 400 °C with a rate of 5 K/min at a starting $H_2$ pressure of 6 bar. We note that crushed into the pieces as cast alloy was not able to absorb reasonable amount of hydrogen at such experimental conditions. In order to obtain completely saturated by hydrogen samples, as cast alloy must be hydrogenated and dehydrogenated at least one cycle. Fig. 1 presents kinetic curves of the first hydrogenation of the RS1000 and RS3000 ribbons. Both samples exhibit an incubation period preceding the onset of hydrogen absorption, when the surface oxide layers present on the ribbons were penetrated by hydrogen gas. The incubation time was around 7 min for the RS1000 ribbons and 12 min for the RS3000 ribbons. The reason for such a difference is in a fact that the surface to volume ratio for the RS3000 ribbons is higher than that for the RS1000 sample. During the active hydrogen absorption, both samples were saturated with hydrogen before reaching 150 °C. The hydrogen absorption capacity of the Ti–V ribbons was lower than that of the arc melted pre-alloy. Indeed, the as cast alloy absorbed 3.95 wt.% H, while $Ti_{0.8}V_{0.2}$ RS1000 and $Ti_{0.8}V_{0.2}$ RS3000 absorbed 3.75 wt.%

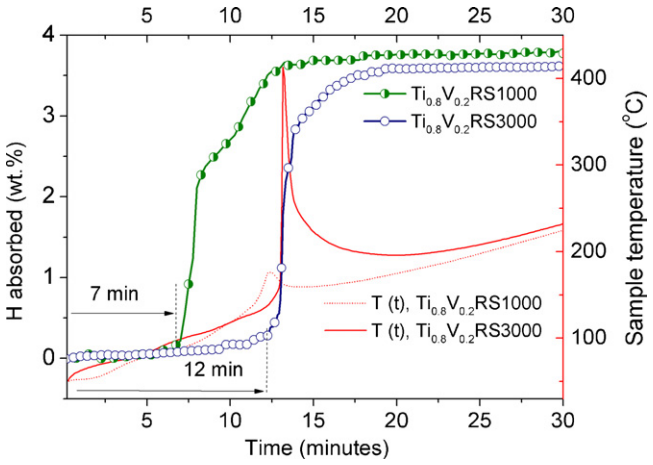


**Fig. 1.** First hydrogenation of the melt-spun $Ti_{0.8}V_{0.2}$ ribbons. Ribbons were heated from RT to 400 °C at the initial hydrogen pressure of 6 bar. Sample temperature $T(t)$ during hydrogen absorption shows a significant exothermic effect of hydrogenation.

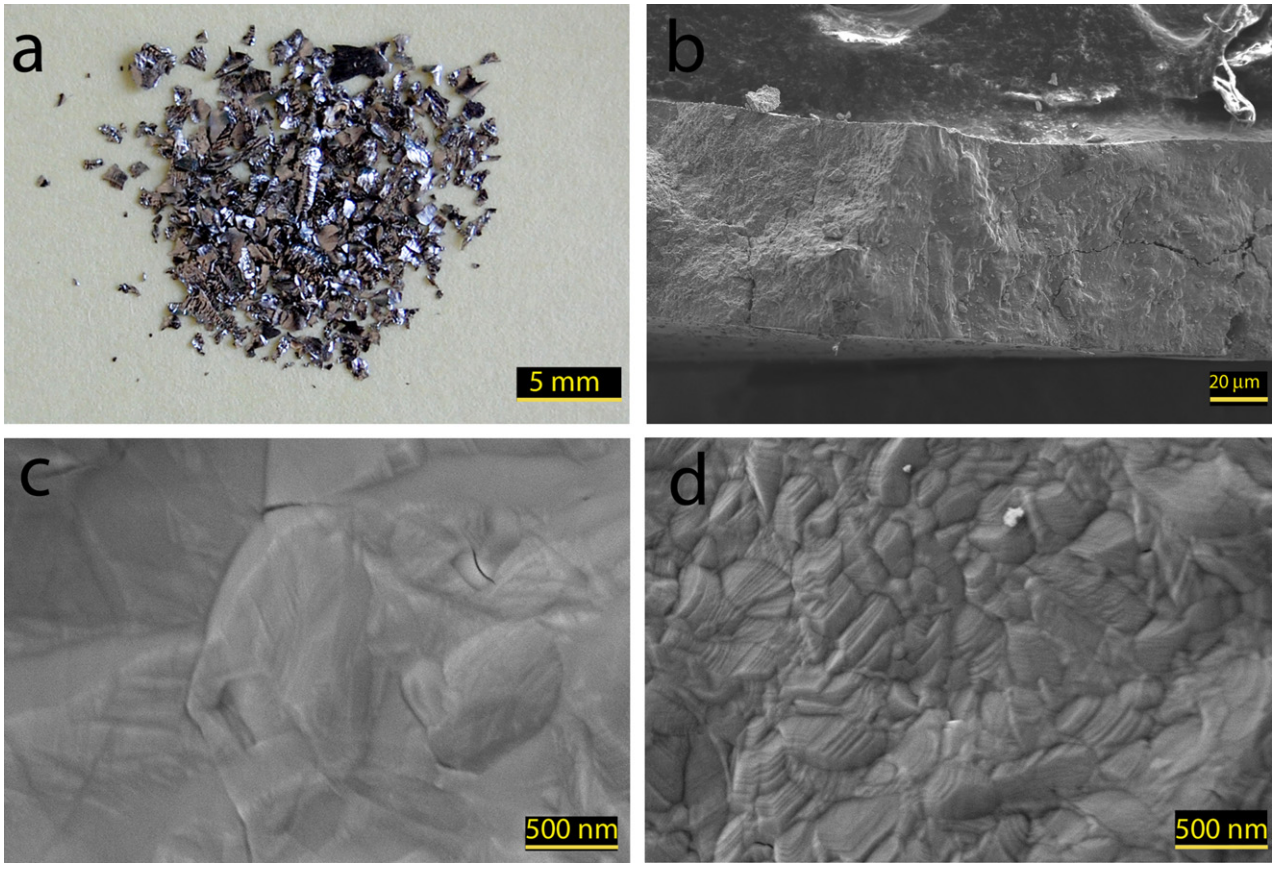


**Fig. 2.** (a) General view of the hydrogenated ribbons. (b) Morphology of a hydrogenated ribbon (cross-section view). (c) Microstructure of the hydrogenated $Ti_{0.8}V_{0.2}$ RS1000. (d) Microstructure of the hydrogenated $Ti_{0.8}V_{0.2}$ RS3000.

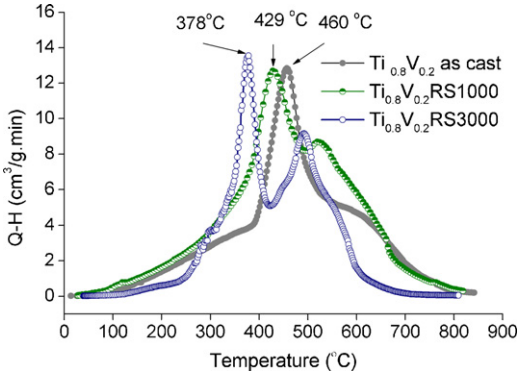


**Fig. 3.** TDS spectra of the $Ti_{0.8}V_{0.2}$ hydrides. Heating rate 5 K/min.

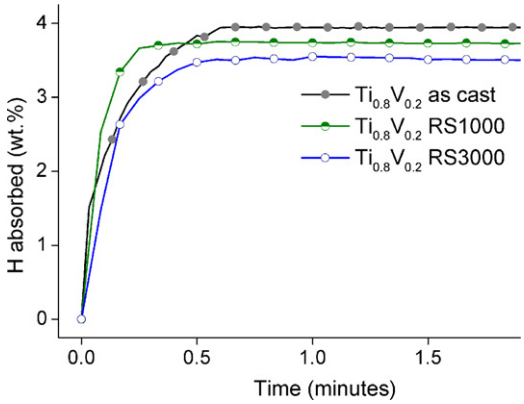


**Fig. 4.** Third hydrogenation kinetics of the melt spun ribbons. Hydrogenation was performed at 6 bar hydrogen and 30 °C.

H, and 3.50 wt.% H, respectively. An increase in the surface-to-volume ratio in the RS3000 sample could be a possible reason for its decreased hydrogen storage capacity. This indicates that effective for hydrogen absorption volume of the sample is slightly reduced as a consequence of the surface oxidation during the melt spinning.

The morphology of the ribbons after the hydrogenation was studied by SEM and is shown in Fig. 2. The hydrogenated ribbons were not completely pulverized; instead, most of the hydrides were in the form of small, millimetre range, flakes, as shown in Fig. 2a. The flakes remain intact even after the third hydrogenation cycle, despite some cracks become visible (Fig. 2b). Such behaviour is beneficial for hydrogen storage materials, contrasting to a usual morphology changes on hydrogenation yielding the powdered hydrides. Fig. 2c and d shows microstructure of the hydrogenated $Ti_{0.8}V_{0.2}$ RS1000 and $Ti_{0.8}V_{0.2}$ RS3000 ribbons, respectively. SEM study revealed that the $Ti_{0.8}V_{0.2}$ RS1000 hydride had an average grain size of around 500 nm while the grain size of the $Ti_{0.8}V_{0.2}$ RS3000 hydride was only 200 nm. These values show that the alloy grain size affects the hydride grain size, as the grain boundaries in the alloy act as a nucleation sites for the hydride formation during the hydrogenation process [13].

The effect of the melt spinning on the dehydrogenation properties of the corresponding hydrides is illustrated in Fig. 3, where the TDS spectra of the hydrogenated prealloy and melt spun-based hydride sample are given. The hydrogenated ribbons desorbed hydrogen with two well-resolved steps. The first step proceeds in the temperature range 378–457 °C and most likely corresponds to a transformation from a dihydride δ-$Ti_{0.8}V_{0.2}H_{2-x}$ into a monohydride β-$Ti_{0.8}V_{0.2}H_x$. The second hydrogen evolution peak at above 500 °C indicates hydrogen desorption from β-$Ti_{0.8}V_{0.2}H_x$ to form β-$Ti_{0.8}V_{0.2}$, and is similar to the process in the Ti-H system [14]. From these TDS spectra, it can be inferred that rapid solidification results in a thermal destabilization of the hydride. Indeed, the main peak of the hydrogen TDS curve for the hydride of $Ti_{0.8}V_{0.2}$ RS3000 is located at lower temperature than that of the $Ti_{0.8}V_{0.2}$ RS1000 and as cast alloy hydrides. The decrease is 79 °C for $Ti_{0.8}V_{0.2}$ RS3000 as compared to the as cast alloy. Another important parameter provided by the TDS spectra is the decomposition rate during the hydrogen desorption. The highest hydrogen decomposition rate was observed for the hydrogenated $Ti_{0.8}V_{0.2}$ RS3000 ribbons. This is an indication of the enhancement of the kinetics of the hydrogen desorption, which well correlates with the smaller hydride grain size in the hydrogenated $Ti_{0.8}V_{0.2}$ RS3000. It is also worth to mention a clear separation of two H desorption peaks present on the TDS curve for the $Ti_{0.8}V_{0.2}$ RS3000 hydride.

Subsequent hydrogenation was performed at 30 °C and 6 bar $H_2$. Fig. 4 shows that all alloys are able to rapidly form the hydrides. All samples were saturated by hydrogen within less than 1 min. The hydrogen absorption capacity changes in interval between 3.95 wt.% H (as cast alloy) and 3.50 wt.% H for the $Ti_{0.8}V_{0.2}$ RS3000, with an intermediate value of 3.75 wt.% H for the $Ti_{0.8}V_{0.2}$ RS1000 hydride. These values are slightly lower than those observed during the first hydrogenation. Despite that increased solidification rate decreases the maximum hydrogen capacity, hydrogen absorption kinetics of the rapidly solidified alloys is excellent.

The *ex situ* synchrotron XRD was used to evaluate the phase composition of the alloys and their corresponding hydrides. When $Ti_{0.8}V_{0.2}$ alloys were saturated by hydrogen, they formed an FCC dihydride δ-$Ti_{0.8}V_{0.2}H_x$ with a $CaF_2$ type crystal structure (space group $Fm\bar{3}m$). Based on the measurements of the volumetric changes during the present hydrogenation experiments, the value of $x$ was estimated to be in the range from 1.76 to 1.99, as related to the synthesis conditions. Typical powder diffraction spectra of

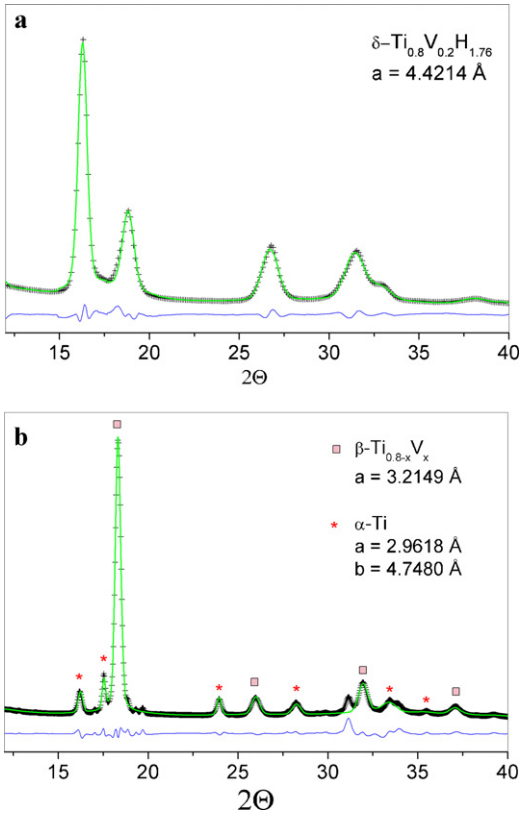


**Fig. 5.** SR XRD pattern of (a) $Ti_{0.8}V_{0.2}$ RS3000 hydride; $R_{wp}$ = 4.41% and $R_p$ = 3.34%; (b) $Ti_{0.8}V_{0.2}$ RS3000 dehydrogenated sample; $R_{wp}$ = 11.65% and $R_p$ = 6.12%.

**Table 1**
Crystallographic data for the hydrogenated and dehydrogenated $Ti_{0.8}V_{0.2}$. $R_{wp}$ and $R_p$ are in the ranges 4.41–11.65% and 3.34–6.12%, correspondingly.

| Sample | As cast (arc melted) | $Ti_{0.8}V_{0.2}$ RS1000 | $Ti_{0.8}V_{0.2}$ RS3000 |
|---|---|---|---|
| Hydrogenated alloy | δ-$Ti_{0.8}V_{0.2}H_{1.99}$<br>($Fm\bar{3}m$)<br>$a$ = 4.4340(7) Å | δ-$Ti_{0.8}V_{0.2}H_{1.86}$<br>($Fm\bar{3}m$)<br>$a$ = 4.4198(9) Å | δ-$Ti_{0.8}V_{0.2}H_{1.76}$<br>($Fm\bar{3}m$)<br>$a$ = 4.4214(3) Å |
| Dehydrogenated alloy | β-$Ti_{0.8}V_{0.2}$ ($Im\bar{3}m$)<br>$a$ = 3.231(1) Å<br>wt. fraction = 0.97<br>α-Ti ($P6_3/mmc$)<br>$a$ = 2.953(5) Å<br>$b$ = 4.705(3) Å<br>wt. fraction = 0.03 | β-$Ti_{0.8}V_{0.2}$ ($Im\bar{3}m$)<br>$a$ = 3.250(1) Å<br>wt. fraction = 0.87<br>α-Ti ($P6_3/mmc$)<br>$a$ = 2.965(1) Å<br>$b$ = 4.755(2) Å<br>wt. fraction = 0.13 | β-$Ti_{0.8}V_{0.2}$ ($Im\bar{3}m$)<br>$a$ = 3.214(1) Å<br>wt. fraction = 0.88<br>α-Ti ($P6_3/mmc$)<br>$a$ = 2.961(1) Å<br>$b$ = 4.748(2) Å<br>wt. fraction = 0.12 |

$\delta - Ti_{0.8}V_{0.2}H_x$ and its respective dehydrogenated alloys are presented in Fig. 5. The hydride unit cell parameters are in the ranges of 4.42–4.43 Å. From XRD data, the dehydrogenated alloy consists of β-$Ti_{0.8}V_{0.2}$ (space group $Im\bar{3}m$), α-Ti, and small amounts of an unidentified phase, most likely titanium–vanadium oxide. Table 1 lists the crystallographic data of the hydrides and their corresponding dehydrogenated alloys. Presence of titanium metal in the dehydrogenated melt spun ribbons could be explained by a phase separation during the melt spinning process as well as trend to the element segregation in the Ti–V alloys during the hydrogen absorption–desorption cycling [15–17]. When titanium separates from the $Ti_{0.8}V_{0.2}$ solid solution, the titanium fraction in the solid solution phase decreases, so its composition becomes enriched by vanadium, $Ti_{0.8-x}V_{0.2+x}$. A reduction of titanium content in the $Ti_{0.8}V_{0.2}$ decreases the temperature of the main desorption peak in the TDS spectrum. However, comparison of the data presented in Table 1 shows that the amount of titanium phase is almost identical in both melt spun alloys. Thus, it is reasonable to suggest that the decrease in $Ti_{0.8-x}V_{0.2+x}H_{2-y}$ TDS main peak temperature of hydrogen desorption from the RS3000 hydride as compared to the data for the RS1000 is due to a smaller crystallites size for the former hydrogenated alloy.

We note that the unit cell parameters of the hydride $Ti_{0.8}V_{0.2}$ RS1000 and $Ti_{0.8}V_{0.2}$ RS3000 are close to each other despite of the differences in the hydrogen storage capacity of these two materials. Since the lattice parameters depend on the amount of hydrogen in the hydrides [18,19], we conclude that some parts of the rapidly solidified alloys are inactive to hydrogen uptake. As previously mentioned, $Ti_{0.8}V_{0.2}$ RS3000 has a higher specific surface area than $Ti_{0.8}V_{0.2}$ RS1000 and, therefore, the content of the surface oxide is increased. Thus, the apparent hydrogen absorption capacity of the $Ti_{0.8}V_{0.2}$ RS3000 is lower than that of the $Ti_{0.8}V_{0.2}$ RS1000.

## 4. Conclusions

Melt spinning technique has been used to synthesize the $Ti_{0.8}V_{0.2}$ nanostructured ribbons. An increased wheel spinner velocity gives a higher solidification rate and affects the hydrogenation properties. Microstructural and hydrogen Thermal Desorption Spectroscopy studies showed that improved kinetics of hydrogen exchange as well as thermal destabilization of the hydrides can be gained as an outcome of the application of the melt spinning synthesis process. This favourable modification of the hydrogen sorption properties illustrates the advantages of applying the melt spinning technique when producing the hydrogen storage alloys, despite the observed slight decrease in hydrogen storage capacities.

## Acknowledgments

The authors thank the Norwegian Research Council Norway and Statoil for their financial support. We appreciate a help from Dr. Jan Petter Mæhlen. A skilful assistance from the personal of Swiss-Norwegian Beam Lines during the SR XRD experiments is gratefully acknowledged.

## References

[1] K. Nomura, E. Akiba, J. Alloys Compd. 231 (1995) 513–517.
[2] K. Kubo, H. Itoh, T. Takahashi, T. Ebisawa, T. Kabutomori, Y. Nakamura, E. Akiba, J. Alloys Compd. 356–357 (2003) 452–455.
[3] T. Kabutomori, H. Takeda, Y. Wakisaka, K. Ohnishi, J. Alloys Compd. 231 (1995) 528–532.
[4] X. Yu, Z. Wu, F. Li, B. Xia, N. Xu, Appl. Phys. Lett. 84 (2004) 3199.
[5] K. Iwase, Y. Nakamura, K. Mori, S. Harjo, T. Ishigaki, T. Kamiyama, E. Akiba, J. Alloys Compd. 404 (2005) 99–102.
[6] X.B. Yu, Z. Wu, N.X. Xu, Phys. B: Condens. Mat. 344 (2004) 456–461.
[7] H. Arashima, F. Takahashi, T. Ebisawa, H. Itoh, T. Kabutomori, J. Alloys Compd. 356–357 (2003) 405–408.
[8] H. Itoh, H. Arashima, K. Kubo, T. Kabutomori, K. Ohnishi, J. Alloys Compd. 404–406 (2005) 417–420.
[9] P. Pei, X.P. Song, J. Liu, G.L. Chen, X.B. Qin, B.Y. Wang, Int. J. Hydrogen Energy 34 (2009) 8094–8100.
[10] Y. Wu, W. Han, S.X. Zhou, M.V. Lototsky, J.K. Solberg, V.A. Yartys, J. Alloys Compd. 466 (2008) 176–181.
[11] H. Jones, Mater. Sci. Eng. 65 (1984) 145–156.
[12] H. Jones, Mater. Lett. 26 (1996) 133–136.
[13] J. Bloch, M.H. Mintz, J. Alloys Compd. 253–254 (1997) 529–541.
[14] C. Borchers, T.I. Khomenko, A.V. Leonov, O.S. Morozova, Thermochim. Acta 493 (2009) 80–84.
[15] S. Ono, K. Nomura, Y. Ikeda, J. Less-Common Met. 72 (1980) 159–165.
[16] B. Nowak, S. Hayashi, K. Hayamizu, O. Yamamoto, J. Less-Common Met. 123 (1986) 75–84.
[17] T. Hagi, Y. Sato, M. Yasuda, K. Tanaka, Jpn. Inst. Met. Trans. 28 (1987) 198–204.
[18] Y. Fukai, The Metal–Hydrogen System, 2 ed., Springer, Berlin, 2005.
[19] V.A. Yartys, V.V. Burnasheva, K.N. Semenenko, Sov. Adv. Chem. 52 (1983) 529–562.